of one of the α branches from the experimental data. An explanation in terms of magnetic breakdown seems most plausible.

The fixed-band model, which considers only the changes due to electron-concentration effects, indicates that the bulk of the dHvA frequency shift is due to the reduction in the number of conduction electrons. This may explain why the model fits alloys so well, but despite this, the other effects of alloying also appear to be adequately represented in the model: The full calculation shows considerable improvement over the simple fixed-band-model results.

ACKNOWLEDGMENTS

The authors gratefully acknowledge the assistance of Professor J. P. G. Shephard and of Dr. Derek Parsons in the early stages of this work; the helpful suggestions of Professor R. W. Stark, Professor L. M. Falicov, and Professor P. Soven; and the cooperation of Dr. G. London in the preparation of alloy samples and in providing alloy lattice parameters.

*Work supported in part by the Air Force Office of Scientific Research under Grant No. AF AFOSR 536-66 and 69-1637 to Case Western Reserve University, Cleveland, Ohio.

†Present address: Department of Physics, University of Connecticut, Storrs, Conn. 06268.

‡NASA Predoctoral Trainee. Present address: Department of Physics, The Louisiana State University, Baton Rouge, La.

[1]J. H. Tripp, P. M. Everett, W. L. Gordon, and R. W. Stark, Phys. Rev. 180, 669 (1969), to be referred to as I.

[2]P. M. Everett, thesis, Case Western Reserve University, 1968 (unpublished); Cryogenics (to be published).

[3]W. A. Harrison, *Pseudopotentials in the Theory of Metals* (Benjamin, New York, 1966).

[4]O. P. Gupta, Phys. Rev. 174, 668 (1968).

[5]L. Nordheim, Ann. Physik 9, 607 (1931).

[6]R. G. Chambers, Proc. Phys. Soc. (London) 88, 701 (1966).

[7]See Fig. 2 of I for caliper designations.

[8]N. E. Alekseevski and V. S. Egorov, Zh. Eksperim. i Teor. Fiz. 55, 1153 (1968) [Soviet Phys. JETP 28, 601 (1969)].

PHYSICAL REVIEW B VOLUME 2, NUMBER 6 15 SEPTEMBER 1970

Occupied Band Structure of Cu: Soft-X-Ray Spectrum and Comparison with Other Deep-Band-Probe Studies

R. C. Dobbyn, M. L. Williams, J. R. Cuthill, and A. J. McAlister
Institute for Materials Research, National Bureau of Standards, Washington, D. C. 20234

(Received 4 March 1970)

We report a new measurement of the soft-x-ray $M_{2,3}$ emission spectrum of Cu, using improved experimental techniques. Previously unreported fine structure was observed in the spectrum. Although exact correction for satellite and subband overlap and self-absorption effects is not yet possible, careful consideration has been given to them, with the result that the M_3 band profile can be resolved from the accompanying structure in a plausible way. Its features can be taken with reasonable confidence to be characteristic of the true M_3 profile. Comparison is made with the complementary L_3 soft-x-ray profile, with band-theoretical estimates of both experimental x-ray profiles, and with the results of ultraviolet-photoemission, x-ray–photoemission, and ion-neutralization measurements. These comparisons favor a single-particle description of the occupied bands of Cu.

I. INTRODUCTION

Increasingly detailed and realistic calculations of the band structure of the 3*d* metals are becoming available. Notable success has been achieved in predicting the results of experiments which probe electronic structure at the Fermi level. However, such work yields only a limited indication of the validity of single-particle band theory.[1] A full test requires experimental data covering the full range of occupied band structure. To this end, optical, soft-x-ray (SXS), ultraviolet-photoemission (UPS), x-ray–photoemission (XPS), and ion-neutralization (INS) spectroscopies are available. Until recently, only crude agreement has been found among these various experiments, and between such experiments and theory. Many often marked discrepancies have occurred. Even now, it is not completely clear to what extent these arise from purely experimental difficulties on the one hand, or to dif-

ferences in such matters as transition probabilities and the role of many-body effects on the other. Progress is being made, however. Recent UPS studies on carefully prepared samples of Cu[2] and Ni[3,4] show marked correlation with band-theoretical estimates of deep-lying density-of-states structure. In the present work, we have employed state-of-the-art advances in vacuum spectroscopy in a new measurement of the $M_{2,3}$ soft-x-ray emission spectrum of Cu, and have been able to establish the existence of fine structure in the spectrum. The results support a single-particle description of Cu.

The M_3 band is extracted from the $M_{2,3}$ spectral complex in a plausible way and compared with the complementary L_3 emission spectrum.[5] Both experimental profiles are compared with band-theoretical estimates of them.[6,7] These comparisons suggest that single-particle excitations make the dominant contribution to the observed spectra, with multiparticle effects warping them to a significant but not destructive extent. Finally, the M_3 profile is compared with the results of UPS,[2] XPS,[8] and INS[9] studies of Cu. Exact correlation is found between partially resolved structure in the SXS profile and the more prominent structure observed in the recent UPS work. Rough qualitative agreement is found with the XPS and INS results. The over-all agreement found among the experiments, and between the experiments and theory, indicates that the single-particle picture can yield a realistic description of the electronic structure of Cu well off the Fermi level. But detailed agreement between these experiments and theory is not yet seen. Much more extensive theoretical analysis than is presently available of the roles played by transition probabilities and multiparticle effects is required.

II. EXPERIMENTAL

The sample was a polycrystalline Cu rod, of stated purity 99.999%. Before mounting in the spectrometer, the sample was machined lightly and washed, first in acetone, then absolute alcohol. Prior to washing, a Pt-Pt 10% Rh thermocouple was peened into a narrow hole bored in the sample. Measurements were carried out using 2.5-keV electron-beam excitation, at (580± 5) °C, at sample-chamber pressure ranging from 4 to 9 $\times 10^{-8}$ Torr. The spectrometer (a glass-grating grazing-incidence Rowland mount, using photoelectric detection) has been described elsewhere.[10,11] Certain details of operation are pertinent to the present discussion. Grazing electron-beam incidence and 90° x-ray takeoff angle were employed to minimize self-absorption.[10] The instrument was calibrated by using the known spectrometer drive geometry, locating the first- and second-order Al $L_{2,3}$ emission edges, and assigning them wavelength values determined from the $L_{2,3}$ absorption edge data of Codling and Madden.[12] This is a rough procedure, but quite adequate for the purposes of this work. Data were taken by sweeping the spectrum continuously, recording total count over successive constant-time intervals. Many sweeps were then summed to enhance the signal-to-noise ratio. The standard counting error in the raw spectrum (70% confidence level) ranges from 1.1 to 0.7%. This degree of statistical assurance was achieved at the expense of instrumental resolution, which we estimate to be 0.35 eV at the spectral peak. Contamination of the sample appeared to be minimal. Very weak carbon emission bands were detected in first and second order. This presumably arises from deposition of cracked-vacuum-pump oil vapor on the sample by the electron beam. As noted above, this contamination is quite weak, and should produce no significant effect on the Cu spectrum, either by order overlap or chemical combination. Of concern also are oxygen contamination and cold-work structural distortion by machining. Both of these problems appear to be solved by the elevated temperature at which the measurements were made. Recovery curves for Cu[13] indicate that, at 580 °C, cold-work distortion should be almost completely relieved in 30 min, while our sample was maintained at this temperature for at least 2 h before measurements were started. It seems unlikely that any significant amount of oxide could be present on the sample surface at the temperature and pressure used here. The optical properties of Cu are quite sensitive to the presence of thin oxide films on the surface. Roberts[14] has found from a series of optical measurements that oxide can be removed from polycrystalline bulk Cu by heating to 277 °C in a pressure of 10^{-5} Torr. His work does not rule out the possibility of a residual complete or partial monolayer, nor can the possibility of oxygen diffusing into the sample be precluded. Significant evolution of gas occurs as the sample is heated, however, suggesting that very little of the oxygen initially present in the oxide layer diffuses in.

III. DATA ANALYSIS

The function one hopes to extract from a measurement of this type is the single-hole M_3 emission profile. The measured spectrum, shown in Fig. 1, is a complex of overlapping M_2 and M_3 bands and satellites, the entire complex overlying a background continuum consisting of bremsstrahlung reflected in first and higher orders and radiation diffusely scattered by the grating. In general,

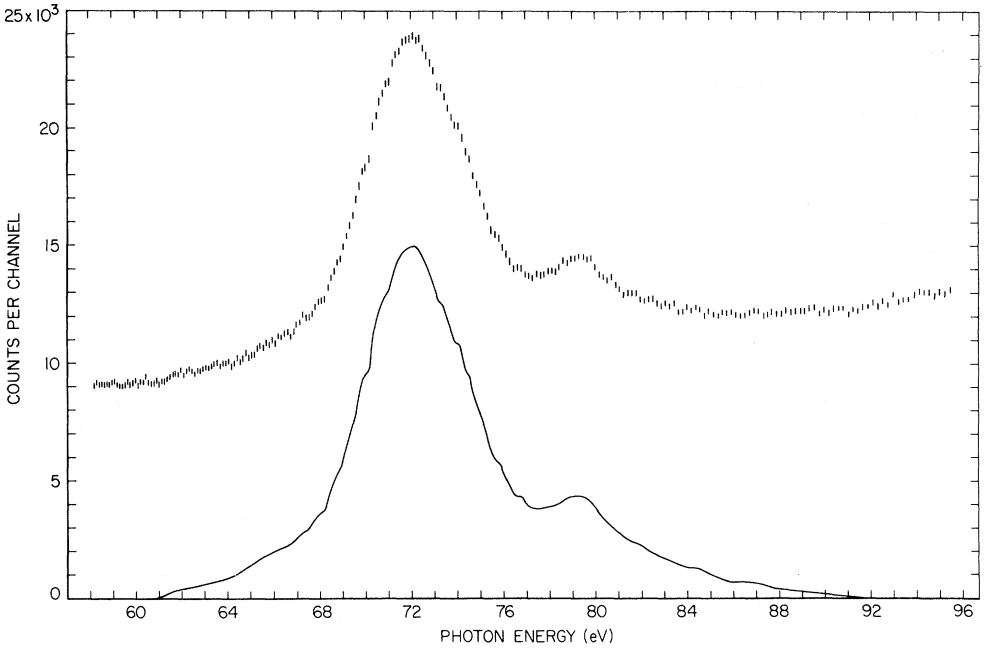

FIG. 1. Upper curve, the uncorrected $M_{2,3}$ spectrum of Cu. Bar length represents 70% confidence level. Lower curve, the smoothed spectrum, corrected for background.

the spectrum may be more or less distorted by self-absorption. However, for reasons presented in detail elsewhere,[10,15] we believe that our use of grazing electron-beam incidence and 90° x-ray takeoff angle reduces self-absorption to a negligible level, while yielding sufficient penetration to ensure bulk behavior. We estimate an effective emission depth of about 150 Å in this experiment.

The first correction made on the spectral complex is subtraction of the background. We have adopted the usual procedure of scanning the spectra of neighboring elements which have no characteristic structure in the region of the Cu $M_{2,3}$ complex at the same exciting voltage. In this way, a "universal" background curve was constructed. This curve was then fitted to the Cu data, above and below the spectral complex, and subtracted off. The lower of the two curves in Fig. 1 is the difference between the fitted background curve and a fair curve drawn through the raw data in a manner consistent with the indicated counting error.

To proceed with the task of extracting the M_3 profile from the background-corrected complex of Fig. 1, let us first ask what structures are to be expected. The most obvious are the M_2 and M_3 profiles, overlapping because the spin-orbit splitting ϵ of the $3p^{1/2}$ and $3p^{3/2}$ inner levels is less than the over-all M_3 bandwidth. We make the reasonable assumption that the remaining structure in the complex consists of two families of Wentzel-Druyvesteyn satellites.[16] For one family, the spectator hole is assumed to reside in the $3p$ shell; for the other, in the valence-conduction band. For a spectator hole in the $3p$ shell, we expect the mean energy of the satellite structure to exceed that of the parent by roughly the difference in binding energy of a $3p$ electron in the element under study and that of the element 1 at. no. higher. Treating the two-hole configuration in the intermediate-coupling scheme,[17] neglecting core contraction, we anticipate five possible initial states: a triplet P with splittings $\frac{2}{3}\epsilon, -\epsilon/\sqrt{3}$, and $-\frac{2}{3}\epsilon$; and singlet S and D with splittings $\frac{4}{3}\epsilon$ and $-\frac{2}{3}\epsilon$, respectively. The corresponding satellite structure should be dominated by those members of the family arising from transitions into the p-like initial states, since they alone sample the dominant d component of the valence-conduction band. As we shall presently see, the upper end of the $M_{2,3}$ complex can be reasonably interpreted with this picture. When the spectator hole resides in the valence band, interpretation is in principle more complex, but in practice far simpler. Considered here are satellites arising from the Auger decays $3p^{1/2} \rightarrow 3p^{3/2}$, v and $3p$, $3p \rightarrow 3p^{1/2}$, v or $3p^{3/2}$, v followed by radiative transitions $3p^{3/2}$, $v \rightarrow v$, v' and $3p^{1/2}$, $v \rightarrow v$, v'. We denote by v a hole in the valence-conduction band. Guidance to the proper handling of these satellites can be gotten from analysis of the experiments of Liefeld,[5,18] who studied the L_3 spectra of Cu and Ni, employing exciting electron-beam voltages just above and just below L_2 threshold. Below L_2 threshold, only the L_3 single-hole radiative transition $2p^{3/2} \rightarrow v$ occurs, while above, the satellite emission $2p^{3/2}$, $v \rightarrow v$, v' is also observed, following the Auger decay $2p^{1/2} \rightarrow 2p^{3/2}$, v. Owing to

the large spin-orbit splitting of the $2p^{1/2}$ and $2p^{3/2}$ levels (15 to 20 eV) we would expect to be able to treat the $2p$, v configuration as spin-orbit split in the intermediate-coupling scheme. This procedure leads to estimated over-all splittings enormously larger than those experimentally observed.[19] It is possible, in fact, to achieve quite fair estimates of the undistorted Ni and Cu L_3 profiles from the L_3-satellite complexes by treating the valence-band satellite structure as a simple image of the parent, shifted up to higher energy. This is illustrated in Fig. 2. It is reasonable to assume that such satellites in the $M_{2,3}$ complex can be treated in the same way. Furthermore, the mean satellite shift cannot exceed the $3p$ spin-orbit splitting ϵ. In view of the L_3 results, and bearing in mind that the mean shift resulting from reduced screening should be roughly equal for the two spectra, we deem it unlikely that the mean shift should be materially less than ϵ, and we therefore adopt the following working picture of the major structures in the $M_{2,3}$ complex. We assume it to consist of 2 sets of 3 bands each:

$$M(E) = [M_3(E) + \alpha_1 M_3(E-\epsilon) + \alpha_2 M_3(E-2\epsilon)] + [\beta_1 M_3(E-\delta-\tfrac{2}{3}\epsilon) + \beta_2 M_3(E-\delta+\epsilon/\sqrt{3}) + \beta_3 M_3(E-\delta+\tfrac{2}{3}\epsilon)] ,$$

where δ is the mean shift of the satellite family with an inner-level spectator hole. Since δ in general is much larger than ϵ (about 10 eV compared to 2 eV), a first estimate of the M_3 profile can be obtained by approximating the low-energy tail of the inner-level spectator hole satellites by suitably scaling the low-energy tail of the main band complex, shifting it up in energy by δ, and subtracting. We then make estimates of ϵ, α_1, and α_2, and solve the expression

$$M_3(E) = \sum_{n=0}^{N} (-1)^n \{\alpha_1^n M(E-n\epsilon) + n_1 \alpha_1^{n-1} \alpha_2 \times M(E-(n+1)\epsilon) + [n(n-1)/2!]\, \alpha_1^{n-2} \alpha_2^2 M(E-(n+2)\epsilon) + [n(n-1)(n-2)/3!]\, \alpha_1^{n-3} \alpha_2^3 M(E-(n+3)\epsilon) + \cdots\}$$

obtained by inverting $M(E) = M_3(E) + \alpha_1 M_3(E-\epsilon) + \alpha_2 M_3(E-2\epsilon)$. ($N = W/\epsilon$, W = width of the lower three-band complex.) The estimate of M_3 so obtained is then used to make a more realistic fit to the high-energy satellite structure, which is then subtracted, and the procedure repeated until an unchanging estimate of M_3 is found. This procedure is obviously rough. Still, the effects of these approximations on the resolved M_3 band appear to be minor. Varying the parameters ϵ, α_1, and α_2 over quite a wide range produces *no* significant change of the resolved M_3 profile in a broad region extending from the bottom of the band to about 1.5 eV below the high-energy edge. Near the edge an uncertainty of about ± 20% (at most) in the amplitude results. The occurrence and location of fine structure are unaffected.

In Fig. 3, we show the M_3 profile of Cu resolved from the smoothed complex of Fig. 1 by the method just described. The particular parameters employed for the solid curve were $\epsilon = 2.0$ eV, $\alpha_1 = 0.5$, and $\alpha_2 = 0.2$. The range of parameters considered was $0.4 \leq \alpha_1 \leq 0.7$, $0.3 \leq \alpha_2 \leq 0.05$, and

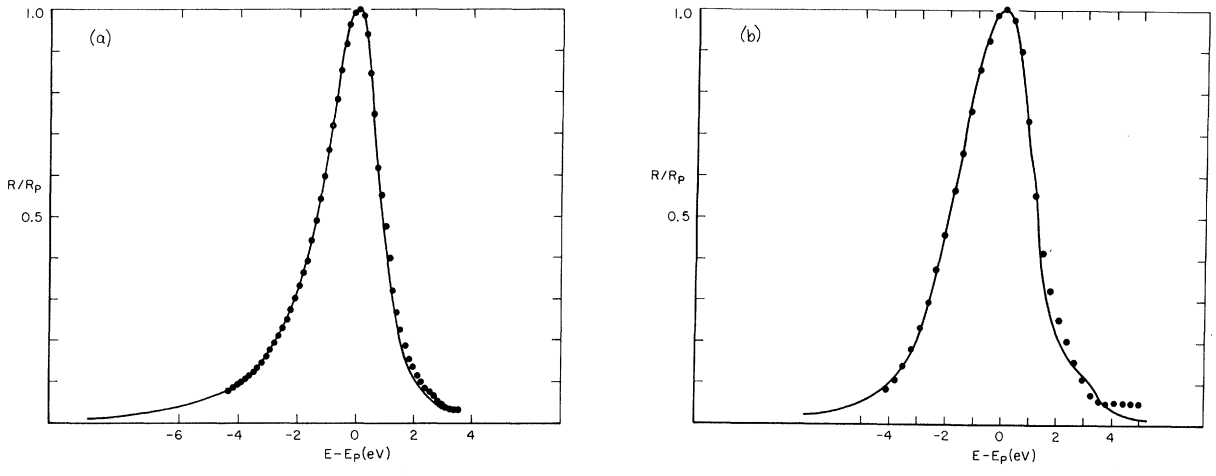

FIG. 2. Solid curves, L_3 profiles of Ni (a) and Cu (b), after Liefeld (Ref. 5). Dotted curves are estimates of L_3, gotten from L_3-valence-band satellite complexes (Refs. 5 and 18) by assuming the valence-band satellite to be a simple image of the L_3 parent, shifted up in energy.

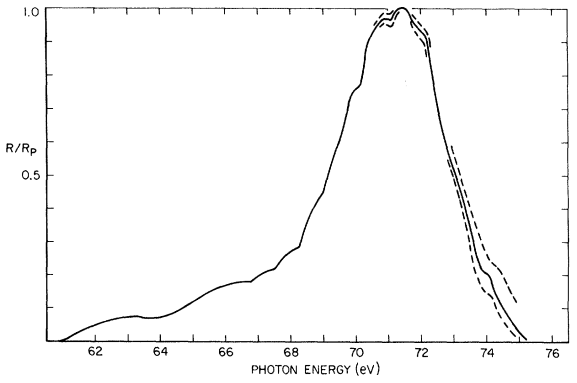

FIG. 3. Cu M_3 profile, solid curve. Dashed curves show the extreme behavior encountered in varying the unfolding parameters.

$2.0 \leq \epsilon \leq 2.4$. The dashed curves in the figure show the extreme behavior encountered.

Some additional support for the value $\epsilon = 2.0$ eV exists. If the $K\beta_{1,3}$ emission line of Cu is assumed to consist of two overlapping Lorentzian lines, with $K\beta_3$ one-half as intense as $K\beta_1$, then ϵ can be estimated from the observed asymmetry index and width at half-maximum[20] to be 2.05 eV.

IV. EARLIER WORK AND THE L_3 SPECTRUM; COMPARISON OF L_3 AND M_3 SPECTRA WITH THEORY

The raw Cu $M_{2,3}$ spectrum shown in Fig. 1 is in very good general agreement with earlier measurements using photographic detection,[21,22] and with the photoelectric detection results of Catterall and Trotter,[23] who presented the average of several strip-chart recorded scans. However, by using photoelectric detection and by summing many scans of the spectrum to enhance the signal-to-noise ratio, we have been able to establish the existence of fine structure in the spectrum. In addition we believe that we have performed a much more reliable unfolding of the M_3 profile from the $M_{2,3}$ spectral complex than has been carried out heretofore.

In Fig. 4, the Cu M_3 profile is compared with the L_3 profile determined by Liefeld.[5] The L_3 curve was recorded at threshold excitation, and is entirely free of self-absorption and satellite distortion. It has been corrected only for background. It should be noted that the resolution of the L_3 measurement is poorer than that of the M_3, owing to a slightly larger inner-level width and the relatively wide spectral window of the crystal spectrometer necessary in the L spectral range. The resulting resolution for the L spectrum from these sources is roughly 1.0 eV, while for the M spectrum reported here, it is 0.4 to 0.5 eV. (The M resolution could be improved. We have used wider slits and larger counting intervals than optimum to enhance the counting rate.) The zero of energy assigned to the L_3 profile is taken from the inflection point of the L_3 absorption edge, as determined by Liefeld.[5] The M_3 spectrum is positioned on the basis of structural correlations between the two profiles. It would be desirable to make a similar absorption edge assignment for the M_3 spectrum, but this is not possible. The $M_{2,3}$ absorption edge is quite broad,[24,25] from 2 to 3 V wide. This situation is apparently due to a delayed onset of oscillator strength, of the type described by Cooper,[26] and observed in Sn by Codling *et al.*[27] and Xe by Ederer.[28] Haensel *et al.*[25] have estimated the partial oscillator sum

$$N_{\text{eff}} = (mcA/2\pi^3 e^2 L\rho) \int_{\omega_1}^{\omega_2} \mu n \, d\omega ,$$

where L is Avogadro's number, A the at. wt, ρ the density, n the real part of the index of refraction, and μ the mass absorption coefficient. Using their own (and supplementary data at lower energies) they estimate $N_{\text{eff}} \approx 6$ at the $M_{2,3}$ edge, indicating that the oscillator strength for the eleven $4s$ and $3d$ electrons is far from exhausted at the mean edge energy of 76 eV. On the other hand, the L_3 edge is as sharp as the experimental resolution permits, and presumably gives a fair estimate of the location of E_F.

While definite structural correlations exist between the L_3 and M_3 profiles, the disparities between them are much more apparent. The M profile is much wider than the L at half-maximum, and in the region below the d hump, where one might expect radiative transitions from band states of dominantly s character, the M is much more intense than the L. This is the general case for heavy $3d$ metals.[29] Qualitatively, such differences are predicted by one-electron theory. They arise

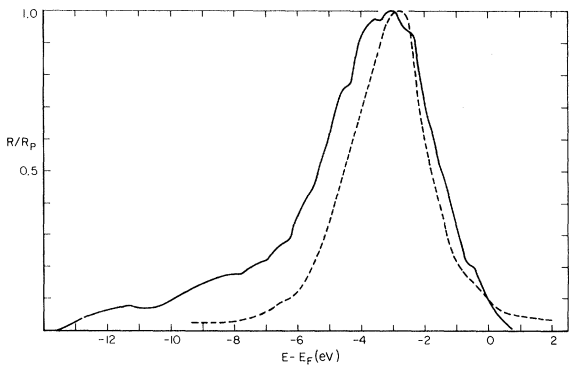

FIG. 4. Comparison of the M_3 and L_3 profiles. The latter was measured at threshold excitation by Liefeld (Ref. 5).

from the fact that, while the $2p$ (for the L) and $3p$ (for the M) inner levels have the same orbital symmetry, the radial wave functions are quite different. The $3p$ radial function is noded; the $2p$ unnoded and more strongly localized than the $3p$. Consequently, they sample the radial components of the band wave functions differently.

One-electron estimates of the emission rate can be made in the following way. If calculations are carried out over a mesh of points $\vec{k}$ in a symmetry subsection of the Brillouin zone, the spontaneous flux of photons per steradian per unit energy R can be estimated by constructing histograms of bar width $2\Delta E$ as follows:

$$R(E_i - E_c) \propto \sum_{\vec{k}} N(\vec{k})\{[E(\vec{k}) - E_c]/[E_0 - E_c]\}^3 \times |\langle \psi_{np} | \vec{r} | \psi(\vec{k}, E)\rangle|^2 D(E) . \quad (1)$$

$E(\vec{k})$ is the eigenenergy of a given state, E_0 the energy at the bottom of the bands, and E_c the energy of the core state. ψ_{np} is the core-state wave function, $\vec{\psi}(k, E)$ a valence-conduction-band wave function. Also,

$$N(\vec{k}) = 2dn(\vec{k})/\sum_{\vec{k}} n(\vec{k}) ,$$

where 2 is the spin degeneracy, d the degeneracy of the given eigenstate, and $n(\vec{k})$ the number of points in the star of $\vec{k}$. Finally, $D(E) = 1$ if $E_i - \Delta E \le E < E_i + \Delta E$, and 0 elsewhere.

We now make a one-center estimate of the square of the dipole matrix elements, using band wave functions calculated by the augmented-plane-wave (APW) method,[30] and tabulated free-atom wave functions for the inner level.[31] Integrations are carried out only over the APW sphere (centered on a lattice site, with radius equal to one-half the nearest-neighbor distance). This truncation is justified by inspection of the atomic core wave functions which, for the heavy $3d$ metals, have negligible probability density outside this sphere. In this approximation

$$|\langle \psi_{np} | \vec{r} | \psi(\vec{k}, E)\rangle|^2 = \tfrac{16}{3}\pi \sum_{\vec{g}_i, \vec{g}_j} C_i C_j [G^2_{np,s} j_0(k_i A) \times j_0(k_j, A) + 2G^2_{np,d} j_2(k_i A) j_2(k_j A) P_2(\cos\theta_{ij})] \quad (2)$$

for spin-degenerate bands. Here $\vec{g}$ is a reciprocal-lattice vector, $\vec{k}_i = \vec{k} + \vec{g}_i$, the C_i's are coefficients of the normalized band eigenfunction expanded in augmented plane waves, A is the APW sphere radius, $j_l(k_i A)$ is an lth-order spherical Bessel function, θ_{ij} is the angle between two vectors $\vec{k}_i$ and $\vec{k}_j$, and $P_2(\cos\theta_{ij})$ is the second-order Legendre polynomial. The quantities $G_{np,l}$ are functions only of energy, and are defined by

$$G_{np,l} = \int_0^A dr\, r^3 R_{np}(r) R_l(r)/R_l(A) ,$$

where R_{np} is the inner-level radial wave function and R_l the radial wave function of the lth orbital component of the band wave function.

It is convenient to express these results in terms of orbital state densities

$$n_l(E) = \sum_{\vec{k}} N(\vec{k}) w_l(\vec{k}, E) D(E) , \quad (3)$$

with $w_l(k, E)$ defined by

$$\sum_l w_l + w_{pw} = \int_{\text{cell}} \psi^*(\vec{k}, E)\psi(\vec{k}, E)\, d\tau = 1 .$$

The l sum is equal to the integral over the APW sphere; the plane-wave term w_{pw} equals the integral over the volume between the sphere and the atomic cell boundary. It is easily shown that

$$w_l(\vec{k}, E) = 4\pi(2l+1) \sum_{i,j} C_i C_j P_l(\cos\theta_{ij}) j_l(k_i A) j_l(k_j A) \times \int_0^A dr\, r^2 [R_l(r)/R_l(A)]^2$$

and

$$w_{pw}(\vec{k}, E) = \sum_{i,j} C_i C_j \left(\Omega \delta_{ij} - \frac{4\pi A^2 j_1(k_{ij} A)}{|\vec{k}_{ij}|} \right) ,$$

where Ω is the atomic cell volume.

Substituting this and Eq. (3) into Eqs. (1) and (2) yields

$$R(E_i - E_c) \propto [M^2_{np,s} n_s(E) + \tfrac{2}{5} M^2_{np,d} n_d(E)] \times [(E - E_c)/(E_0 - E_c)]^3 \quad (4)$$

for the photon flux per unit energy, where

$$M_{np,l} = \int_0^A dr\, r^3 R_{np}(r) R_l(r, E) ,$$

with the band-orbital radial wave function normalized over the APW sphere volume. Clearly, the L and M spectra should differ if the M's do.

The R_l's can be evaluated by numerical integration of the Schrödinger equation for a given potential. The M's are then obtained by numerical integration. We have estimated the energy dependence of the M's for Fe, Ni, and Cu using atomic wave functions tabulated by Herman and Skillman,[31] and various crystal potentials; in particular, for Cu, the Chodorow potential[32] was used. The results for Cu are typical (though the strength of the behavior increases from Fe to Cu), and are illustrated in Fig. 5, where we have plotted the various $M^2_{np,l}$ as a function of energy. Both $M^2_{2p,d}$ and $M^2_{3p,d}$ are scaled to unity near the bottom of the conduction band. $M^2_{2p,s}$ and $M^2_{3p,s}$ are plotted to correct relative scale. The $3d \rightarrow 2p$ transition probability is sharply enhanced with respect to the $3d \rightarrow 3p$ probability as one goes from the bottom to the top of the filled bands. Thus, upon normalizing both spectra at peak intensity, the L-spectrum d

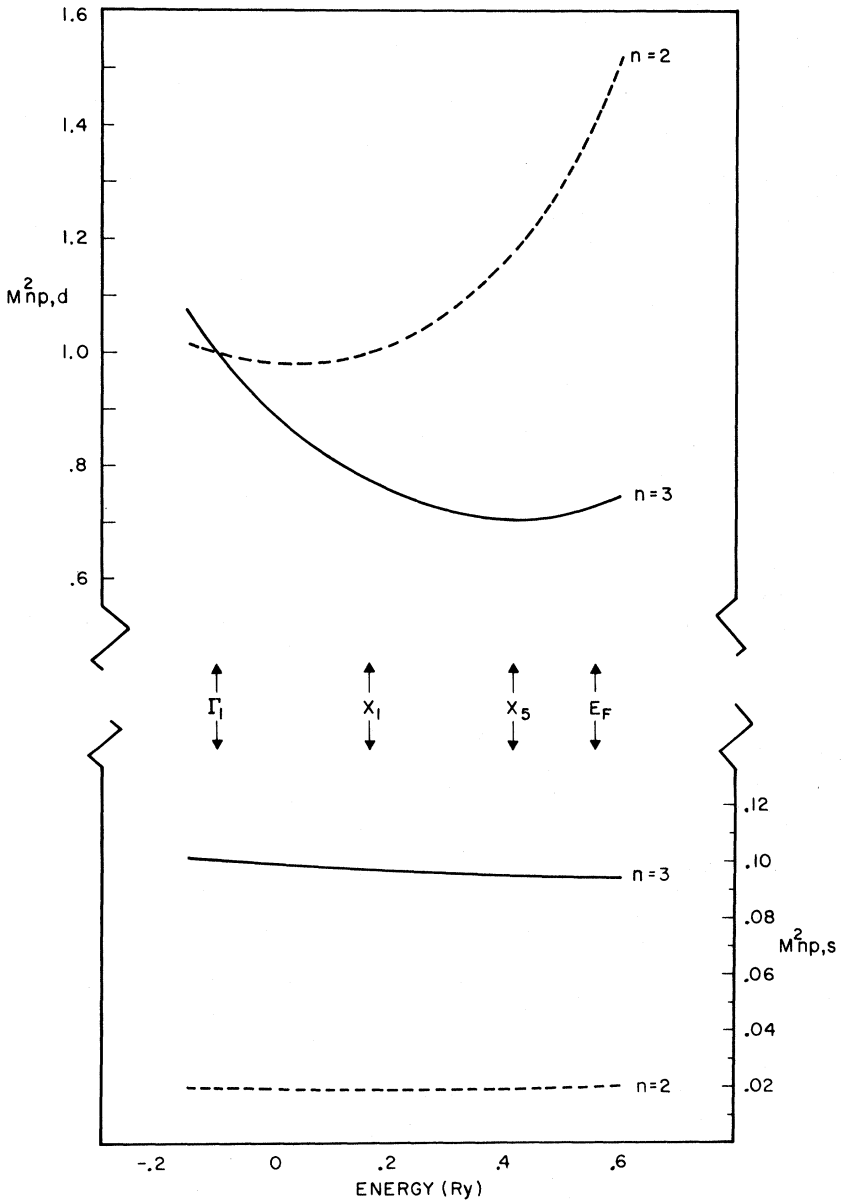

FIG. 5. Radial factors $M^2_{np,l}$ entering the one-electron estimates of the L and M emission spectra, calculated from the Chodorow potential.

hump should appear narrower than the M. We have noted this effect before,[10] making estimates from radial d orbitals for Fe published by Wood.[33] Not considered in this earlier work were differences in $4s \rightarrow 2p$ and $4s \rightarrow 3p$ transition probabilities. Inspection of Fig. 5 shows them to be significant. For an M spectrum, the s component should be much more intense relative to the d than for the L: for Cu, about six times more intense. Similar results have recently been found for Cu by Goodings and Harris.[6,34] These effects at first appear to provide a natural explanation for the disparities between the L and M spectra of Cu and other heavy $3d$ metals. We shall presently see, however, that while qualitatively correct, they are not sufficiently strong to bring theory and experiment into agreement. The E^3 term in Eq. (4), important only for the M spectrum, largely negates the d enhancement of the L spectrum. Furthermore, band-theory estimates of n_0 show it to be far too weak relative to n_2 for the s enhancement of the M spectrum to have much of an effect on a one-electron estimate of the spectra. Still, these considerations may provide clues to a correct interpretation of the the L and M profiles, a question we will return to after some detailed comparison with theory.

Before making comparison with band-theory estimates of the L_3 and M_3 profiles, we make one

adjustment of the measured M_3 profile. In Fig. 6, the unfolded M_3 profile is shown, the zero of energy being the Fermi energy as estimated above. Arrows indicate the calculated positions of the top and bottom of the d bands and the bottom of the conduction band relative to the Fermi energy, as calculated by Burdick[32] and Snow.[7] Of particular interest is the fact that the low-energy tail of the M_3 band extends well below the estimated bottom of the conduction band. The well-known low-energy tailing[35] of x-ray band spectra undoubtedly plays a role here, but note the distinct hump, occurring between -10.5 and -13.0 eV. This structure peaks at about -11.3 eV, 8.2 eV below the point of peak intensity. Some caution is needed here, since we are dealing with structure only slightly larger than the statistical noise. The presence of this hump is certain, but we cannot be sure of its exact shape. Consider now the observation of a characteristic electron-energy-loss peak for Cu at 7.6 ± 0.3 eV,[36] which is identified by optical studies[37] as the free-electron plasma resonance, lowered somewhat by d-band polarization. Consider further the prediction[38] and observation[39] of plasmon satellites in the light metals, weak images of the main band (washed out at higher energies), shifted down in energy by the plasmon energy. The intensity of the observed hump in the raw Cu spectrum is about 3% of the peak main-band intensity, about that seen for uncorrected simple-metal spectra. The larger intensity of Fig. 6 results from our first-order correction for the changing resolution in energy of our spectrometer. We therefore identify this bump as a plasmon satellite, and to obtain a rough estimate of the single-particle contribution to the spectrum, assume the main-band intensity to be zero under it, treat it as an exact image of the main band, and subtract it off. The dashed curve of Fig. 6 shows the main-band tail so corrected.

In Fig. 7, we compare the corrected experimental M_3 profile with two one-electron estimates. Fig. 7(a) shows the recent work of Goodings and Harris,[6,34] based on the Chodorow potential. Fig. 7(b) shows a hybrid estimate, arrived by combining n_0 and n_2 estimated by Snow from his first-principles calculation[7,40] with M values calculated in the present work from the Chodorow potential. (The band structures calculated by Snow and by Burdick, who used the Chodorow potential, differ only slightly, so no significant inconsistency should result from this procedure.) In each case, the lower curve is the corrected experimental M_3 profile. The upper curve is the calculated one-electron profile, with no allowance made for spectrometer, inner level, or energy-dependent lifetime smearing. The middle curve shows the result of folding

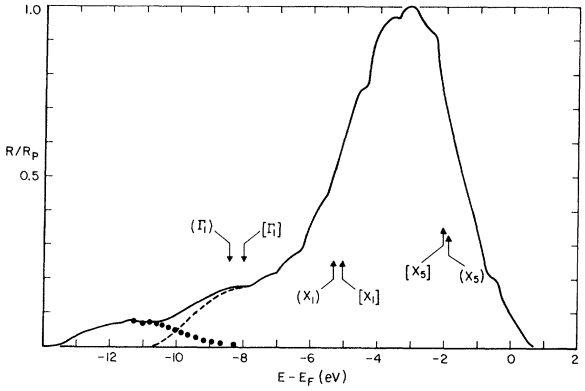

FIG. 6. M_3 profile, corrected for the presence of the plasmon satellite. Arrows indicate the positions of the top and bottom of the d bands, and the bottom of the conduction band, as calculated by Burdick (Ref. 32) (parentheses) and Snow (Ref. 7) (brackets).

in an energy-dependent smearing function. Lorentzian shape is assumed, with width equal to 0.4 eV at E_F to approximate the effects of the instrument and the inner level, and increasing to 1.4 eV at the bottom of the conduction band, to approximate the effect of final-state hole lifetime, according to the prescription

$$\Gamma(E) = \Gamma(E_F) + \Gamma_B[1 - (E - E_0)/(E_F - E_0)]^2 .$$

The second term on the right-hand side is Blokhin and Sachenko's[41,42] approximation to Landsberg's expression for final-state breadth in the electron-gas approximation. Inspection of Fig. 7 shows heartening agreement in the region of the d hump, particularly in the case of the Goodings-Harris estimate. Disturbing features, however, are the excess intensity of the measured curve below the d hump, and the very slow decrease in intensity above the d hump. This latter difficulty is present in the L_3 spectrum as well, and more than a simple underestimate of level broadening appears to be involved. This is indicated by the generally satisfactory degree to which d-hump structure survives folding with the assumed smearing function, as well as the suggestion of partially resolved structure at -1.4 eV in both the measured L and M spectra. It is possible that virtually bound states are generated by the inner-level vacancy. There is evidence of this same sort of behavior in the Ni M_3 spectrum as well, as we shall note in Sec. V.

In Fig. 8, we compare measured L_3 and M_3 spectra (bottom curves) with smeared calculated curves (middle) from the sources used for Fig. 7. For the L spectrum, $\Gamma(E_F)$ is taken to be 1.0 eV, to allow for a slightly larger inner-level width and

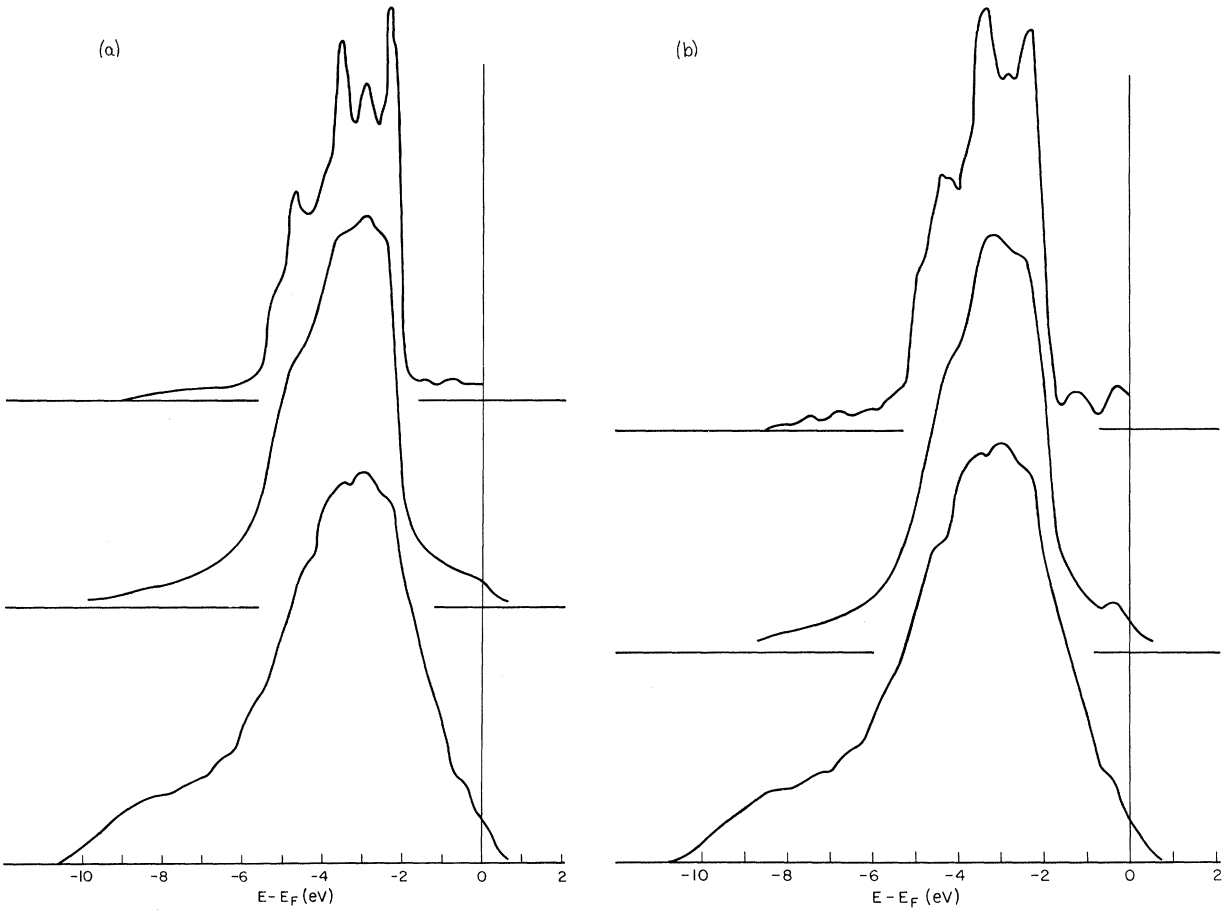

FIG. 7. Comparison of the plasmon-corrected M_3 profile with two one-electron estimates. In each case, the lower curve is the experimental profile. Upper curve is the one-electron estimate, and the middle curve, the one-electron estimate folded with the energy-dependent smearing function discussed in the text. (a) shows the work of Goodings and Harris (Refs. 6 and 34) and (b) the orbital densities of Snow (Refs. 7 and 40) combined with the radial factors of Fig. 5.

the wider spectral window of the crystal spectrometer used in determining it. As noted and explained above, the qualitatively correct one-electron predictions of differences in the L and M profiles are not strong enough to produce the experimentally observed differences. These one-electron estimates are subject to the legitimate criticism that they take no account of charge polarization by the initial-state vacancy. They may be regarded as reliably predicting the distribution in energy of the phase-shifted Bloch states and differences in the way the orbital components of these states are sampled by the different inner levels. However, the predicted amplitudes of the orbital components may be quite erroneous. The following heuristic explanation for the observed L and M profile discrepancies was tested. It is possible that in the screening process, large positive s-wave phase shifts occur, with small negative d-wave shifts. Since an excess local charge of 1 must be attracted, the s components of the spectra could be considerably enhanced relative to the d. While an unknown degree of energy dependence could occur in such enhancement, a simple test was made by assuming constant s/d enhancement factors. This tends to improve agreement with experiment, as the top curves of Fig. 7, for which a fivefold enhancement was assumed, show. But again, the hypothesized effect appears to be much too weak. A proper many-body estimate of such factors as screening and level broadening would be most desirable, but at present, appears to be impossible. The formalism developed by Glick, Longe, and Bose[43] is applicable to Cu in principle, but knowledge of the complex wave number and frequency-dependent dielectric function is needed for its application,

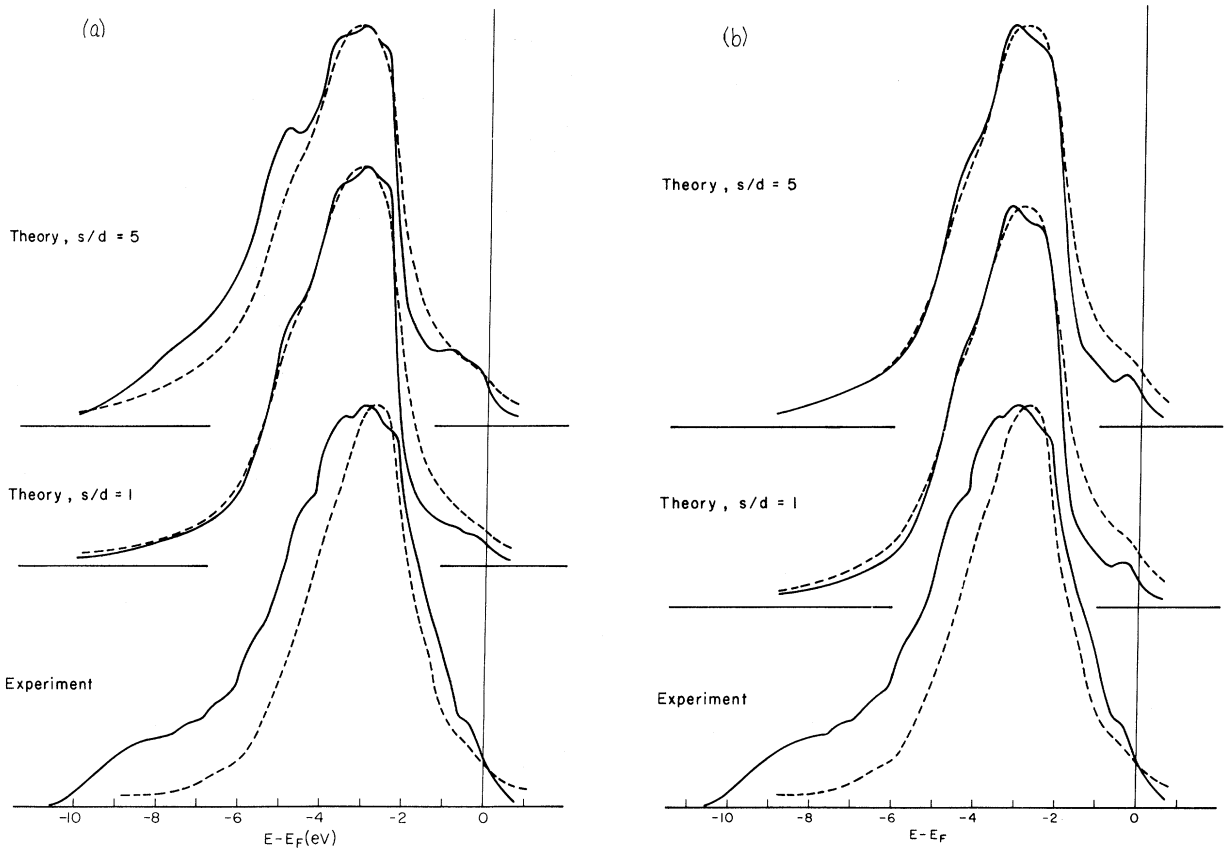

FIG. 8. Comparison of the measured and calculated M_3 and L_3 profiles. In both cases, the lower curves are the experimental profiles of Fig. 4. Middle curves are one-electron estimates folded with the energy-dependent smearing functions described in the text. Upper curves are similarly smeared, but an attempt has been made to account for screening effects by assuming the s part to be enhanced relative to the d by a factor of 5. (a) is based on the work of Goodings and Harris (Refs. 6 and 34) and (b) on the work of Snow (Refs. 7 and 40).

and so far, theory is not able to construct this function for complex metals.

The structural correlations noted here between theoretical predictions with each other, and in turn with the experimental L_3 and M_3 profiles together with agreement of the experimental profiles with the results of other deep-band techniques to be considered in Sec. V, suggest the general validity of a single-particle interpretation. The discrepancies noted may cautiously be attributed to many-body effects which warp the single-hole profiles in not too gross a way. However, the present state of many-body theory does not permit numerical estimate of such warping.

V. COMPARISON WITH OTHER DEEP-BAND-PROBE RESULTS

In Fig. 9, the corrected M_3 profile is compared with the results of other experimental deep-band studies of Cu: the INS unfold function of Hagstrum and Becker,[9] the XPS profile of Fadley and Shirley,[8] and the UPS optical density of states of Cu, recently determined by Krolikowski and Spicer[2] on Cu samples prepared under ultraclean conditions. In each case, the zero of energy is the Fermi energy as estimated by the authors. The dotted portion of the UPS curve represents less certain data obtained from cesiated samples.[44] Each curve has been normalized at peak value.

In making this comparison, it must be born in mind that different excitation mechanisms and transition probabilities are at play. UPS and XPS share the common mode of optical excitation from the ground state, although final states differ. In comparing the XPS and UPS results, it is encouraging to note that the slight low- and high-energy shoulders of the former lie just above the latter's low-energy hump and high-energy d-band edge, while its peak lies just above the slight UPS peak at -3.8 eV. A puzzling aspect of the XPS result

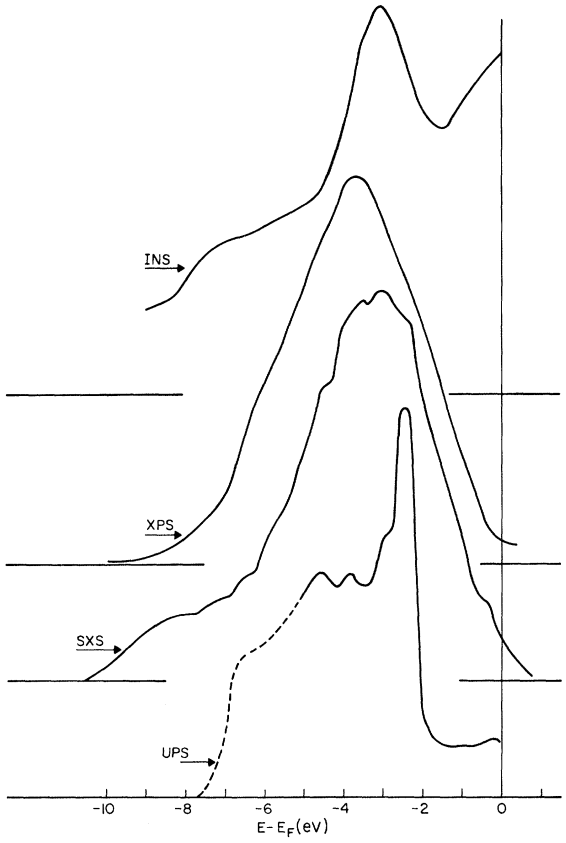

FIG. 9. Comparison of the results of several deep-band probe studies of Cu. Each curve normalized at peak value. UPS after Krolikowski and Spicer (Ref. 2); SXS, present work; XPS after Fadley and Shirley (Ref. 8); INS after Hagstrum and Becker (Ref. 9).

is the fact that the total resolution seems a good deal poorer than the 1.0 eV estimated by the authors. The most striking feature of this comparison is the agreement between the partially resolved structure in the SXS d hump and the more prominent structure in the UPS hump.

Recent analysis of the ion-neutralization process[45] indicates that it occurs at or just outside the sample surface. The INS unfold function reflects the *local* state density and wave functions at the position of the exciting atom. Although in general, it may not be directly connected with the bulk electronic structure for Cu, we note significant points of agreement between INS and the other techniques. If we tentatively assume the Cu INS unfold function to reflect the bulk state density, modified by local wave-function character, then the top and peak of the d hump agree well with the other techniques. If the slight inflection at -6 eV can be construed as the bottom of the d hump, then the over-all width of the INS d hump is in fair agreement as well. Continuing in this vein, one might construe the low-energy shoulder of the INS curve as locating the bottom of the conduction band. We would then assume it to fall at roughly -8.5 eV (bearing in mind the over-all sharpness of the d hump, and assuming this degree of resolution to hold lower in energy as well), while the M_3 low-energy structure is consistent with a conduction-band bottom of, roughly, -9.0 eV.

The over-all picture that emerges is roughly that of one-electron band theory: a full d-band complex extending from -2.0 to roughly -5.5 eV, overlapping a broad conduction band extending to -8.0 or -9.0 eV below E_F. The structural correlation noted between the SXS and UPS results, and in turn, between these experimental results and theory can be construed as support for the validity of a one-electron theory. Closer theoretical study of these various experiments is much needed, however.

A final observation in this section is made in Fig. 10, where the M_3 profiles of Cu and paramagnetic Ni[10] are compared. Owing to their common crystal structure, and the fact that Ni has but one fewer valence-conduction electron than Cu, one would expect correlations in their electronic structure, and if the one-electron interpretation is valid, in their M_3 profiles as well. As Fig. 10 shows, within the d hump this expected correlation does indeed exist. Note also the slight bump on the high-energy edge of the Ni profile. This is suggestive of the similar poorly resolved structure which appears to broaden the high-energy edge of the Cu d hump. These features might arise from a virtual bound state generated by the inner-level vacancy.

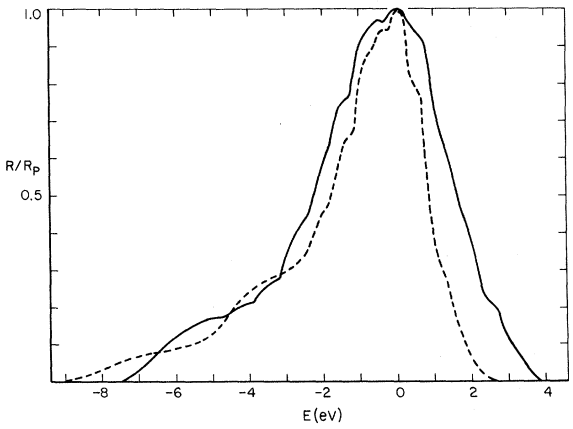

FIG. 10. Comparison of Cu (solid) and Ni (Ref. 10) (dashed) M_3 profiles, positioned to show the structural correlation in the d hump.

In Ni, the state appears to occur above the Fermi level, but could be frequently populated in the sudden production of the inner level. If sufficiently long lived and of proper symmetry, it could then contribute to the observed spectrum.

VI. SUMMARY

We have taken advantage of state-of-the-art advances in vacuum-spectrometry techniques to remeasure the $M_{2,3}$ soft-x-ray emission profile of pure Cu. The existence of previously unobserved fine structure was established. The M_3 single-hole profile was resolved from the $M_{2,3}$ spectral complex in a plausible way, and compared with theoretical estimates of the profile, and with the results of other deep-band probe measurements. A degree of over-all agreement was noted, which tends to support a one-electron description of this heavy $3d$ metal. Certain discrepancies were noted as well, which appear to be attributable to many-body effects which warp the experimental profile to a significant but not too severe degree. Some rationalization of this interpretation has been given, but at present no rigorous treatment of the effects of the electron-electron interaction on the soft-x-ray emission process in complex metals is possible.

ACKNOWLEDGMENTS

We thank Dr. R. E. Watson for several helpful discussions and for a critical reading of the manuscript. Thanks are also due Dr. E. C. Snow, Dr. D. A. Goodings, and Dr. R. Harris for communication of their results prior to publication, and to Dr. W. E. Spicer for enlightening correspondence.

---

[1]Some pertinent references for the $3d$ metals are: E. C. Snow, T. J. Waber, and A. C. Switendick, J. Appl. Phys. 37, 1342 (1966); L. Hodges, H. Ehrenreich, and N. D. Lang, Phys. Rev. 153, 754 (1966); E. C. Snow, *ibid.* 171, 785 (1968); T. L. Loucks, *ibid.* 139, A 223 (1965). An extensive list of references has been given by A. J. Freeman, J. Appl. Phys. 40, 1386 (1969).

[2]W. F. Krolikowski and W. E. Spicer, Phys. Rev. 185, 882 (1969).

[3]D. E. Eastman and W. F. Krolikowski, Phys. Rev. Letters 21, 623 (1968).

[4]T. A. Callcott and A. U. MacRae, Phys. Rev. 178, 966 (1969).

[5]R. J. Liefeld, in *Soft X-Ray Band Spectra*, edited by D. J. Fabian (Academic, New York, 1968), p. 133.

[6]D. A. Goodings and R. Harris, Phys. Rev. 178, 1189 (1969); J. Phys. C 2, 1808 (1969).

[7]E. C. Snow, Phys. Rev. 171, 785 (1968); and (private communication).

[8]C. S. Fadley and D. A. Shirley, Phys. Rev. Letters 21, 980 (1968).

[9]H. D. Hagstrum and G. E. Becker, Phys. Rev. 59, 572 (1967).

[10]J. R. Cuthill, A. J. McAlister, M. L. Williams, and R. E. Watson, Phys. Rev. 164, 1006 (1967).

[11]J. R. Cuthill, Rev. Sci. Instr. 41, 422 (1970).

[12]K. Codling and R. P. Madden, Phys. Rev. 167, 587 (1968).

[13]See, for instance, *Metals Handbook*, edited by T. Lyman (American Society for Metals, Cleveland, 1948), p. 260.

[14]S. Roberts, Phys. Rev. 118, 1509 (1960).

[15]J. R. Cuthill, R. C. Dobbyn, A. J. McAlister, M. L. Williams, Phys. Rev. 174, 515 (1968).

[16]See, for example, E. H. S. Burhop, *The Auger Effect* (Cambridge U. P., Cambridge, England, 1952); F. R. Hirsh, Rev. Mod. Phys. 14, 45 (1942).

[17]E. U. Condon and G. H. Shortley, *The Theory of Atomic Spectra* (Cambridge U. P., Cambridge, England, 1935), Chap. 11.

[18]We are indebted to Professor Liefeld for providing details of his Cu studies, additional to those of Ref. 5. See also, for details of the Ni work, D. R. Chopra, Ph. D. thesis, New Mexico State University (unpublished).

[19]This is a rather surprising result, but it is not the only reported occurrence of weaker than predicted coupling between valence and ion-core shells in the $3d$ metals. Fadley and Shirley (Ref. 8), using the XPS technique, found essentially nil exchange-induced splitting of core levels of Fe and Co.

[20]G. A. Bearden and C. H. Shaw, Phys. Rev. 48, 18 (1935).

[21]J. Clift, C. Curry, and B. J. Thompson, Phil. Mag. 8, 593 (1963).

[22]D. E. Bedo and D. H. Tomboulian, Phys. Rev. 113, 464 (1959).

[23]J. A. Catterall and J. Trotter, Proc. Phys. Soc. (London) 79, 691 (1962).

[24]D. H. Tomboulian, D. E. Bedo, and W. M. Neupert, J. Phys. Chem. Solids 3, 282 (1957).

[25]R. Haensel, C. Kunz, T. Sasaki, and B. Sonntag, Appl. Opt. 7, 301 (1968).

[26]J. W. Cooper, Phys. Rev. Letters 13, 762 (1964).

[27]K. Codling, R. P. Madden, W. R. Hunter, and D. W. Angel, J. Opt. Soc. Am. 56, 189 (1966).

[28]D. L. Ederer, Phys. Rev. Letters 13, 760 (1964).

[29]L. G. Parratt, Rev. Mod. Phys. 31, 616 (1959).

[30]T. Loucks, *Augmented Plane Wave Method* (Benjamin, New York, 1967).

[31]F. Herman and S. Skillman, *Atomic Structure Calculations* (Prentice-Hall, Englewood Cliffs, N. J., 1963).

[32]Chodorow's potential for Cu has been tabulated by G. A. Burdick, Phys. Rev. 129, 168 (1963).

[33]J. H. Wood, Phys. Rev. 117, 714 (1960).

[34]These workers have evaluated the orbital weights of Eq. (3) at 89 points in the reduced fcc zone by inverting the APW matrices and using the Chodorow potential, and then linearly interpolated these solutions onto a mesh of 7000 randomly selected points. We have independently carried out estimates of the orbital weights, using a more accurate interpolation scheme [direct inversion of the APW determinant, using eigenvalues esti-

mated by the interpolation scheme of Hodges, Ehrenreich, and Lang (Ref. 1)] at 505 points in the reduced zone. Agreement between the two estimates was excellent. We employ the results of Goodings and Harris because their more exhaustive sampling of the zone should yield a more realistic estimate of the structure and a more accurate placement of the Fermi level. We note numerical differences between our estimates of the radial matrix elements and theirs. These differences are not large, and probably arise from their different choice of core wave functions.

[35]P. T. Landsberg, Proc. Phys. Soc. (London) A62, 806 (1949).

[36]J. L. Robins and J. B. Swan, Proc. Phys. Soc. (London) 76, 857 (1960).

[37]H. Ehrenreich and H. R. Philipp, Phys. Rev. 128, 1622 (1962).

[38]R. A. Ferrell, Phys. Rev. 28, 184 (1956).

[39]G. A. Rooke, Phys. Letters 3, 234 (1963).

[40]We are indebted to Dr. Snow for private communication of his estimates of the orbital densities from his first-principles band calculation. His calculations were carried out over 89 points in the reduced zone. Results were brought to self-consistency. The local Slater exchange approximation was used, with an arbitrary strength factor of $\frac{5}{6}$ employed to yield better agreement with UPS data.

[41]M. A. Blokhin and V. P. Sachenko, Izv. Akad. Nauk. SSSR, Ser. Fiz. 24, 397 (1960).

[42]This may be a fairly realistic estimate. The insensitivity of *d* electrons to Auger excitation in INS suggests that they might be similarly inoperative here. The strength of the surviving *d*-band structure in Fig. 7 suggests that this is the case.

[43]A. J. Glick, P. Longe, and S. M. Bose, in *Soft X-Ray Band Spectra*, edited by D. J. Fabian (Academic, New York, 1968), p. 319; S. M. Bose, Ph. D. thesis, University of Maryland (unpublished).

[44]W. E. Spicer (private communication). See also, D. E. Eastman, J. Appl. Phys. 40, 1387 (1969).

[45]H. D. Hagstrum, J. Res. NBS 74A, 433 (1970).

PHYSICAL REVIEW B VOLUME 2, NUMBER 6 15 SEPTEMBER 1970

Spin-Disorder Scattering in Iron- and Nickel-Base Alloys

F. C. Schwerer and L. J. Cuddy
Edgar C. Bain Laboratory for Fundamental Research,
United States Steel Corporation Research Center, Monroeville, Pennsylvania 15146
(Received 16 March 1970)

The electrical resistivities of iron-base alloys with Cr, W, Mn, Ru, Co, Ni, Si, or Ge solutes, and of nickel-base alloys with Cr, Fe, Cu, or Pd solutes were measured from 4.2 °K to above the Curie temperatures θ. The solute resistivities $\rho_r(T)[=\rho_{\text{alloy}}(T)-\rho_{\text{host}}(T)]$ were found to be strongly temperature dependent. Above ~ 300 °K, the temperature dependence of $\rho_r(T)$ reflects changes in the electronic structure or in the scattering processes associated with the solutes and is related to changes in the magnetic order. The solute resistivities above 300 °K were found to be in reasonable agreement with a spin-disorder model which explicitly involves the moments localized at the solute sites. Agreement with the well-known Mott band model for ferromagnetic effects in transport properties was not as satisfactory. An essential feature of the analyses of the data involved comparing resistivities of alloy and host corresponding to the same degree of magnetic order. This was accomplished by assuming the ferromagnetic effects in the resistivity scaled as T/θ. The experimental results support the validity of this assumption.

I. INTRODUCTION

It is well known that for metals the electronic transport properties are closely related to the magnetic state. In particular the resistivities of the ferromagnetic transition elements iron and nickel exhibit unusually strong temperature dependences in the temperature ranges in which the magnetic order changes significantly (cf. Figs. 1 and 2). There have been two general approaches to understanding these phenomena.[1-4] In the first approach, a band model, the unusual temperature dependence is associated with increases in the electron *d* states available for scattering as the spontaneous magnetization decreases. In the second approach, disordered magnetic moments are considered to act as additional scattering centers for conduction electrons, and the temperature dependence of the resistivity reflects changes in the degree of magnetic order.

A means of determining whether spin-disorder scattering or the band mechanism is more appropriate for describing the resistivity of a ferromagnetic metal on the basis of qualitative experimental features is provided by studies of the resistivities of dilute alloys.[1-4] The following argument by Coles[1] illustrates the difference in the effects of solutes on the resistivity for the spin-disorder and